Journal of Cellular Biochemistry Supplement 39:25–35 (2002)

Molecular Imaging of Regional Brain Tumor Biology

A.M. Spence,[1]* M. Muzi,[2] and K.A. Krohn[2]

[1]Department of Neurology, University of Washington School of Medicine, Seattle, Washington 98195
[2]Department of Radiology, University of Washington School of Medicine, Seattle, Washington 98195

Abstract Energy metabolism measurements in gliomas in vivo are now performed widely with positron emission tomography (PET). This capability has developed from a large number of basic and clinical science investigations that have cross fertilized one another. This article presents several areas that exemplify questions that have been explored over the last two decades. While the application of PET with [^{18}F]-2-fluoro-2-deoxyglucose (FDG-PET) has proven useful for grading and prognosis assessments, this approach is less clinically suitable for assessing response to therapy, even though results to date raise very intriguing biological questions. Integration of metabolic imaging results into glioma therapy protocols is a recent and only preliminarily tapped method that may prove useful in additional trials that target DNA or membrane biosynthesis, or resistance mechanisms such as hypoxia. There are exciting future directions for molecular imaging that will undoubtedly be fruitful to explore, especially apoptosis, angiogenesis and expression of mutations of genes, e.g., epidermal growth factor receptor, that promote or suppress cellular malignant behavior. J. Cell. Biochem. Suppl. 39: 25–35, 2002.

Key words: glioma; brain neoplasm; glucose metabolism; oxygen metabolism; PET; lumped constant; radiotherapy

Energy metabolism in gliomas has been investigated in the laboratory for decades, but only recently with the development of positron emission tomography (PET) has it become possible to perform non-invasive measurements in vivo in humans. More questions can now be addressed that probe the molecular events that lead to and sustain brain tumor growth. Tracers for investigating glucose and oxygen metabolism were among the first to be subjected to careful study. This article reviews the field of glioma energy metabolism as measured with PET and concludes with a presentation of several exciting future directions molecular imaging in gliomas will follow.

Our laboratory investigates glioma energy metabolism to improve our understanding of the pathophysiology and response to therapy of these tumors and to use the new knowledge to develop better treatments. Glucose metabolism begins with transport from the serum and continues through the process of phosphorylation catalyzed by hexokinase (HK), one of the most important enzymes controlling the rate of glucose utilization. The product, glucose-6-phosphate (G-6-P) is the starting compound for glycogen synthesis, for the Embden-Meyerhof pathway leading to lactate (glycolysis) or pyruvate and entry to the tricarboxylic acid cycle, and for the pentose shunt (PS). Although malignant brain tumor tissue may show a respiratory quotient as low as 0.70, indicating some use of non-glucose substrates, glucose is the chief source of energy [Allen, 1972].

Isozymes of key enzymes are different in gliomas than normal brain. There is a shift to a greater proportion of HKII and a shift of lactate dehydrogenase (LDH) from LDH1 (heart tetramer) toward LDH5 (skeletal muscle tetramer), a change that favors lactate and NAD + production, since LDH5 is not inhibited by pyruvate [Gerhardt et al., 1967]. High lactate levels in tumors including gliomas have been well-documented. The pentose shunt is not very active in normal adult brain and accounts for only two percent of glucose utilization [Gaitonde et al., 1983]. Its flux is increased in rat glial neoplasms [Spence et al., 1997].

Grant sponsor: NIH; Grant number: CA 42045.

*Correspondence to: A.M. Spence, MD, Department of Neurology (356465), University of Washington, Seattle, WA 98195.

Received 3 October 2002; Accepted 3 October 2002
DOI 10.1002/jcb.10406
Published online in Wiley InterScience (www.interscience.wiley.com).

PET imaging with [^{18}F]-2-fluoro-2-deoxyglucose (FDG-PET) is based on the fact that FDG, similar to glucose, is transported across the blood-brain-barrier and cell membranes and is phosphorylated by HK to FDG-6-phosphate, which accumulates in tissues at a rate proportional to the rate of glucose utilization. FDG-6-P is not metabolized further along the glucose metabolic pathways, but is slowly dephosphorylated. As FDG-PET became available for imaging cancers, it was expected to be useful for grading and estimating prognosis, distinguishing recurrence from radionecrosis and assessing response to therapy. However, the history of FDG-PET for malignant gliomas has been checkered by controversies over the value of quantitative studies involving dynamic imaging and biomathematical modeling versus simpler analysis methods [Di Chiro and Brooks, 1988; Hoekstra et al., 2000].

CLINICAL EXPERIENCE HAS HELPED DEFINE IMPORTANT BIOLOGICAL ISSUES

Prognosis and Grading

Di Chiro and coworkers can be credited with pioneering FDG-PET of gliomas [Di Chiro, 1987]. High grade gliomas contained regions of high FDG uptake and lower grade gliomas lacked these regions. In patients with grade III or IV astrocytic gliomas, FDG uptake correlated with survival [Patronas et al., 1985]. The results of other studies of gliomas with FDG-PET agree. In fact, a recent report claims that FDG-PET is better than pathological grading for determining prognosis in gliomas [Padma et al., 2002].

Response to Therapy

Aside from determining prognosis and grading there is the important question whether changes in glucose metabolism correlate with the response of malignant gliomas to therapeutic interventions. Successful radiotherapy (RT) of a metabolically active tumor would be expected to kill tumor cells and be associated with a reduction of metabolism measured with either FDG or 1-[^{11}C]glucose. To investigate this, we studied patients with malignant gliomas prior to and after they received their initial RT [Spence et al., 2002a]. All patients had quantitative scans with both 1-[^{11}C]glucose and FDG that included dynamic imaging and full compartmental modeling of the data as recommended in a recent European consensus report [Hoekstra et al., 2000]. The patients were imaged within 2 weeks before and/or 1–3 weeks after RT. Fourteen patients were imaged both before and after RT, four only before RT and twelve only after RT. The majority received standard conformal external beam RT plus one or more chemotherapy regimes after RT.

Survival was determined from the date of diagnosis and was also assessed relative to historical data reported by the Radiation Therapy Oncology Group (RTOG) [Curran et al., 1993]. Patients were individually placed in the appropriate RTOG classes by age, neurological status, and histology. The increase (or decrease) in survival (ΔS) relative to the appropriate RTOG class was calculated as:

$$\Delta S = \text{individual patient survival} / \text{median survival for RTOG class} \quad (1)$$

In agreement with other reported series, survival assessed in months after diagnosis or ΔS was shorter with higher preRT metabolic rates; lower MR_{Glc} or MR_{FDG} before RT indicated longer survival (Fig. 1) [Di Chiro, 1987; Holzer et al., 1993].

The results of the studies performed both before and after radiotherapy did not support the hypothesis that tumors which responded to treatment would show reduced metabolism after radiotherapy. An increase in metabolism from before RT to after correlated with longer survival. Conversely, a decrease in metabolism was associated with shorter survival (Fig. 1). A similar finding has been reported for a series of brain tumors, predominantly metastatic, that were treated with stereotactic radiosurgery and were studied with FDG-PET within a week before and 4–5 h after the irradiation [Maruyama et al., 1999].

Comparable results, but involving chemotherapy, were reported on patients with recurrent glioblastoma studied with quantitative FDG-PET before and after a single cycle of BCNU [De Witte et al., 1994]. There was a significant positive correlation between survival and glucose metabolism after BCNU; an increase in tumor metabolism predicted longer survival. It was speculated that this resulted from predominant killing of low energy-consuming cells or stimulation of quiescent cells, either tumor or normal, to become more active metabolically. An additional potential explanation is that

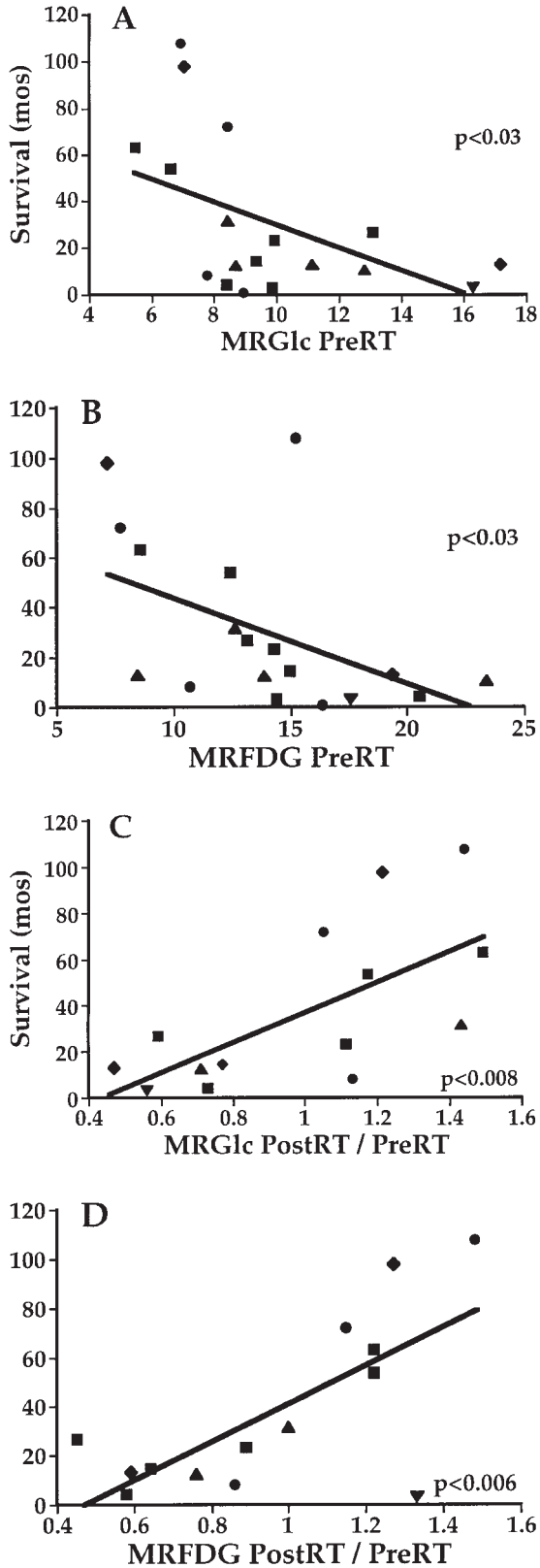

therapy destroys tumor cells leading to an uncrowding effect that allows more active metabolism in surviving normal elements. Within a volume of tissue the ratio and density of normal cells to tumor cells improves, leading to increased regional metabolism.

Laboratory studies have documented that FDG or 2DG uptake in tumors may increase after exposure to chemotherapy or irradiation in vitro or in vivo [Haberkorn et al., 1994; Fujibayashi et al., 1997; Smith et al., 2000]. Increased transport has been considered the leading explanation for this increased uptake.

Increase in MR_{Glc} or MR_{FDG} from before to after radiotherapy that correlates with longer survival could also occur as a result of infiltration of dead and dying tumor regions with metabolically active inflammatory elements [Kubota et al., 1992]. This has been reported following radiotherapy in rats bearing hepatoma tumors implanted in the thigh [Reinhardt et al., 1997]. Autoradiography showed that FDG was concentrated in a tissue layer composed predominantly of fibroblasts and macrophages.

An additional but clearly speculative explanation for increased metabolism after radiotherapy in longer surviving patients is energy consumption for apoptosis. Furuta et al. [1997] and Hasegawa et al. [1997] have reported FDG uptake in irradiated, subcutaneously-transplanted human tumor xenografts in nude mice. At 2, 4, or 6 h after 10 Gy the FDG uptake was doubled in an ependymoblastoma, but did not change in the two other tumors studied. This was associated with a high level of apoptosis in the ependymoblastoma, a tumor known from other experiments to show continuous shrinkage following 10 Gy.

A simpler way to assess response to therapy is to measure metabolism at a single time following the treatment based on a hypothesis that longer survival correlates with lower

Fig. 1. These regression graphs show the data from the studies performed before RT, **A** and **B** (n = 18), and those performed before and after RT, **C** and **D** (n = 14). The symbols show the RTOG prognostic classes of each patient (1 = ◆, 3 = ●, 4 = ■, 5 = ▲, 6 = ▼). A and C graphs are MR_{Glc} and B and D MR_{FDG}. Significance is shown on the individual graphs. A and B show that the patients with the lower metabolic rates before RT had the longer survival; conversely, patients with the higher metabolic rates before RT had the shorter survival. In C and D, the x-axes are the ratio of the PostRT metabolic rate over the PreRT metabolic rate for the two hexoses. The patients whose metabolic rates increased from before RT to following RT showed longer survival.

metabolism. In the 26 glioma cases from our study that had postRT scans, neither MR_{Glc} nor MR_{FDG} correlated with survival or ΔS. No prior studies have looked systematically and quantitatively at the immediate post-radiotherapy time to correlate metabolic rate with outcome. However, examination of FDG uptake of malignant gliomas specifically at the time of clinical and/or radiographic recurrence has proven to be a significant predictor of survival [Barker et al., 1997].

In sum, high MR preceding treatment signifies more aggressive disease and shorter survival. Immediate postRT quantitative PET with either FDG or 1-[^{11}C]glucose does not correlate with length of survival. Comparing pre- to post-treatment measurements for radio-or chemotherapy for primary or metastatic brain tumors show that increases in MR correlate with longer, not shorter survival. These unexpected results could have one of several explanations that require testing in the laboratory. They could be due to decreasing tumor cell density leaving normal cells with higher metabolism, infiltration by inflammatory cells that take up glucose or FDG where tumor cells are dying, or energy consumption for apoptosis of tumor cells in response to RT.

Therapy Planning

Conventional conformal radiotherapy for malignant gliomas consists of 1.8–2.0 Gy fractions daily to a total around 60 Gy. Despite these doses, nearly inevitably there are in-field recurrences, progression, and death. Higher doses, 70–80 Gy, have been explored but with no improvement in survival or local control [Lee et al., 1999]. We examined whether metabolic imaging with FDG-PET could better define the optimal volume of malignant disease in glioblastoma for a high-dose boost. Patients received the conventional dose and an additional 20 Gy in 10 fractions directed at the FDG-PET defined volume of hypermetabolism. Preliminarily, median survival for the group of 40 patients is about 70 weeks. There has been no more radiation toxicity than would be expected from conventional doses. The volume defined by FDG-PET has proven to be an independent prognostic indicator [Tralins et al., in press]. This experimental radiotherapy protocol establishes the feasibility of incorporating PET imaging for targeting the most aggressive region of glioblastoma.

MECHANISTIC STUDIES TEST THE CLINICAL IMAGING PARADIGM

Quantitative Differences Between Glucose and FDG Metabolism in Gliomas: The Lumped Constant (LC)

Because FDG and glucose differ in their rates of transport and phosphorylation, and volumes of distribution in brain tissue, calculation of the glucose metabolic rate (MR_{Glc}) from PET with FDG requires a proportionality constant, the lumped constant (LC_{FDG}), in the operational equation developed by Sokoloff et al. [1977]. The LC_{FDG} represents the ratio of the metabolic rate of FDG (MR_{FDG}) to that of glucose [Sokoloff, 1981]:

$$LC_{FDG} = MR_{FDG}/MR_{Glc} \quad (2)$$

This relationship shows that measurement of the ratio, MR_{FDG}/MR_{Glc}, provides an estimate of the LC_{FDG} and an understanding of how closely FDG approximates quantitatively the glucose metabolic rate. With PET the ratio can be measured regionally.

The LC can also be expressed in terms of the Km and Vmax for FDG and glucose in the HK reaction and the ratio of the volumes of distribution of FDG and glucose (λ) and a ϕ term, assumed to be 1, for the proportion of glucose which, once phosphorylated, is further metabolized. Mathematically,

$$LC_{FDG} = (\lambda/\phi)\left(Km_{Glc} \cdot Vm_{FDG}/Km_{FDG} \cdot Vm_{Glc}\right) \quad (3)$$

$\left(Km_{Glc} \cdot Vm_{FDG}/Km_{FDG} \cdot Vm_{Glc}\right)$ is called the HK phosphorylation ratio (PR)

To measure the LC_{FDG} in vivo we performed sequential dynamic PET imaging with 1-[^{11}C]glucose and then with FDG in 40 malignant glioma-bearing patients [Spence et al., 1998]. MR_{Glc} and MR_{FDG} were estimated for glioma and contralateral brain regions of interest by 3-compartment, 4 rate constant models previously validated for the two hexoses. The LC_{FDG} in gliomas was 1.40 ($\pm$ 0.46, SD) with a range from 0.72 to 3.10 whereas in non-tumor-bearing contralateral brain it was 0.86 ($\pm$ 0.14) with a range from 0.61 to 1.21. In a series of 10 normal subjects the value for brain was 0.89 ($\pm$ 0.08) [Graham et al., 2002].

The findings in a 27-year-old male with a deep left hemisphere glioblastoma multiforme are

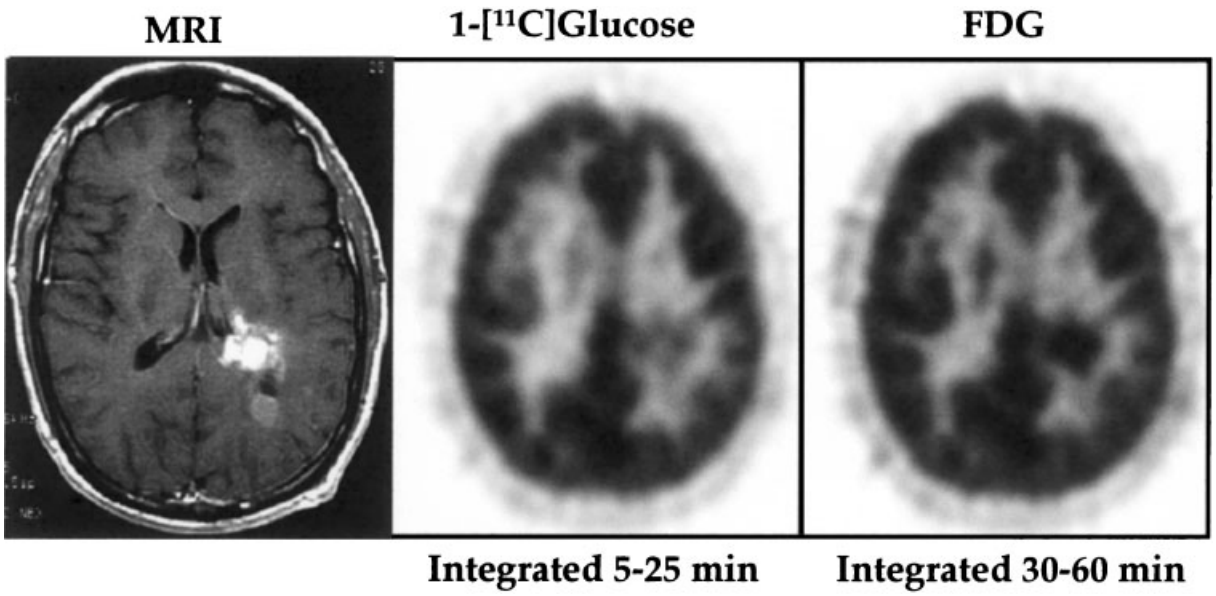

Fig. 2. The tumor MR_{FDG} was 23.4 μmol/100 g/min, MR_{Glc} was 13.4, and LC_{FDG} was 1.75. The contralateral brain MR_{FDG} was 20.9, MR_{Glc} was 22.3, and LC_{FDG} was 0.96.

presented to exemplify these results (Fig. 2). The figure shows his gadolinium-enhanced MRI, 1-[^{11}C]glucose and FDG images all from the same plane. The integrated 1-[^{11}C]glucose image suggests that the glioma was not metabolically more active than cortex whereas the FDG integrated image suggests that it was.

The results from 40 patients confirmed that (a) the glioma LC_{FDG} exceeds that of contralateral brain and may vary from region to region within the tumor, (b) quantitation of the glioma MR_{Glc} with FDG requires knowing the LC_{FDG} specific for the glioma, and (c) the LC_{FDG} of normal brain is much higher than previously reported estimates of about 0.5. FDG-PET studies in which glucose metabolism is calculated with normal brain rate constants and LC_{FDG} overestimate glucose metabolic rate to the extent that the glioma LC_{FDG} exceeds the normal brain LC_{FDG}.

The increased value of the LC in gliomas is likely due to different affinities of HK for the deoxyglucoses (FDG or 2DG) and glucose compared to normal brain, not to an increase of HK activity since these tumors do not have higher HK activity than normal brain [Oudard et al., 1995]. This is further supported by a body of evidence that shows (a) the proportion of HK expressed as HKII is increased in gliomas compared to normal brain which expresses predominantly HKI [Bennett et al., 1978] and (b) HK is less bound to mitochondria in gliomas than in normal brain [Oudard, 1996].

To explore the biological basis for the increased LC_{FDG} in gliomas we measured the kinetics of soluble HK I (predominant in normal brain) and HK II (increased in brain tumors) for the three substrates, glucose, 2-deoxy-D-glucose (2DG), and FDG [Muzi et al., 2001]. Our principal results showed that the $Km_{Glc} < Km_{FDG} \ll$ Km2DG for both HKI and HKII. For HKII, which may reach 20% in human gliomas [Bennett et al., 1978], the Kms for glucose, 2DG, and FDG were all greater than for HK I. Calculation of the phosphorylation ratios for 2DG and FDG for both isozymes showed that the effect of a shift to HK II in tumors would maintain or lower the tumor LC_{FDG}, assuming no change in λ. Thus, it is unlikely that a change in isoenzymes accounts for the observation via FDG-PET of an increased LC_{FDG} in human gliomas.

Compartmentation of HK between mitochondria and cytosol results in a change in HK Km for glucose and FDG but in different ways for the two hexoses [Doenst and Taegtmeyer, 1998]. In human brain tumors approximately 50% of HK is mitochondrially bound compared to 76% for normal brain [Oudard, 1996]. Presumably mitochondrially bound HK is more

efficient for support of oxidative phosphorylation. These observations lead to a hypothesis that in the relationship, $LC_{FDG} \propto Km_{Glc}/Km_{FDG}$, a shift of HKI from bound to unbound would raise Km_{Glc} while a higher proportion of HKII that is not mitochondrially bound would lower Km_{FDG}. Together these changes would raise the LC_{FDG}, all consistent with the tumors having less bound HK, less overall HK activity and a greater proportion of HKII.

Alternatively, the increased uptake of FDG by gliomas may in part result from changes in membrane glucose transport proteins in endothelial cells and/or tumor cells. GLUT 1 is the dominant transporter on normal blood-brain-barrier; normal, reactive and cultured astrocytes; and normal oligodendrocytes. GLUT 3 is the dominant one on neurons and, interestingly, on neoplastic astrocytes and the hyperplastic endothelial cells of gliomas. GLUT 3 transports glucose 7 times faster than GLUT 1. We have examined the relationship, $K1_{DG}/K1_{Glc}$, in intracerebral grafts of rat glioma and normal rat brain [Spence et al., 1988]. Six seconds following simultaneous intracarotid injections of [^{3}H]-DG and 6-[^{14}C]-glucose, the ratio $K1_{DG}/K1_{Glc}$ was 1.1 in glioma and 1.3 in contralateral left hemisphere. Since transport could be rate limiting in the tumor but at the level of the cell membrane rather than the blood-brain-barrier, we measured a relative transport of 1.2 for 2DG versus glucose at the glioma cell membrane level [Spence et al., 1988].

The $K1_{FDG}/K1_{Glc}$ ratios for the main regions of interest from the 40 patients cited above with malignant gliomas were 1.51 ± 0.52 and 1.42 ± 0.36 in gray and white matter, respectively and 1.42 ± 0.45 in glioma [Spence et al., 1998]. While this ratio could be influenced by flow, the ratio in gliomas is equal to or lower than normal brain regions. This provides evidence from modeling that transport is unlikely to lead to a higher LC_{FDG} in gliomas than contralateral brain.

Under certain pathological conditions such as hypermetabolism or hypoglycemia, transport rather than phosphorylation becomes rate-limiting in the uptake of FDG and could be the main determinant of the LC [Crane et al., 1981]. We investigated differences in transport of FDG between malignant and non-malignant cells in vitro [Burrows et al., 2002]. The effects of extracellular glucose concentration over the physiological range expected in brain on FDG uptake was determined as well as the rates of glucose and FDG transport in cells expressing predominantly GLUT-1 or GLUT-3. The extracellular glucose concentration had a greater impact on the rate of FDG accumulation than the relative abundance of the transporter subtypes.

Pentose Shunt

The feasibility of imaging PS glucose (glc) utilization in human gliomas with PET was explored in two rat glioma models in vitro and in vivo by means of glucose radiolabeled in either the C-1 or C-6 position [Spence et al., 1997]. (C-1 of glucose is rapidly converted to CO_2 in the PS whereas C-6 is not. C-1 and C-6 are converted to CO_2 late in the tricarboxylic acid cycle.) In vitro, in rat glioma PS metabolism was only $1.8\% \pm 0.5$ of total glucose utilization. In vivo, rats bearing grafts of gliomas at subcutaneous sites received simultaneous intravenous injections of either 1-[^{11}C]glc and 6-[^{14}C]glc, or 1-[^{14}C]glc and 6-[^{11}C]glc. Retention of C-1 radiolabel relative to C-6 was 5% lower in the two gliomas tested.

An additional group of rats bearing gliomas was exposed to 10 Gy of ^{137}Cs irradiation 4 h before isotope injection in order to deplete NADPH and thereby stimulate the PS. In these animals the C-1 level was 5.6% lower than that for C-6. Mathematical modeling and Monte-Carlo simulations showed that if human gliomas have a similar fractional use of the PS, it should be measurable with PET using sequential studies with 1-[^{11}C]- and 6-[^{11}C]glucose.

IMAGING OF GLIOMA OXYGENATION

Oxygen Metabolism

Oxygen metabolic rate (MRO_2), blood flow (BF), oxygen extraction fraction (OEF), and blood volume (BV) in malignant gliomas have all been examined [Allen, 1972; Rhodes et al., 1983; Wise et al., 1984]. These studies are consistent in showing that oxygen utilization is low relative to normal cortex, despite an adequate supply of oxygen at least macroscopically. Blood flow and blood oxygen levels are adequate to meet the metabolic demands of the tumors. That is, although both MRO_2 and OEF tend to be lower in malignant gliomas, the tissue is not macroscopically ischemic or hypoxic [Wise et al., 1984]. In a study of seven patients with inter-

TABLE I. CBF, MRO_2, and OEF From Glioma and Contralateral Cortex [Rhodes et al., 1983]

Function (Units)	Tumor	Contralateral cortex
CBF (ml/100 ml/min)	32 ± 9	32 ± 5
MRO_2 (ml/100 ml/min)	1.2 ± 0.6	2.8 ± 0.5
OEF	0.21 ± 0.07	0.47 ± 0.05

mediate or high grade gliomas, blood flow in the tumors was the same as in uninvolved brain while MRO_2 and OEF were roughly half (Table I) [Rhodes et al., 1983].

MRO_2 relative to MR_{Glc}, called the metabolic ratio, is reduced in malignant gliomas [Rhodes et al., 1983]. In normal brain the metabolic ratio is 5.2 moles of oxygen/mole of glucose [Baron et al., 1984] while in gliomas it is 1.9 [Rhodes et al., 1983]. A low metabolic ratio indicates that the tissue is breaking down glucose to lactate (glycolysis) and that little oxidative metabolism of glucose is occurring. In the face of adequate blood flow and reduced oxygen extraction in tumors, the reduced metabolic ratio indicates that glycolysis is aerobic rather than anaerobic [Allen, 1972]. Magnetic resonance spectroscopy has shown increased lactate in gliomas, consistent with there being an increased metabolic ratio [Alger et al., 1990; Herholz et al., 1992]. Implanted animal tumors show increased lactate content assessed by a bioluminescence method [Hossmann et al., 1986]. Also, malignant gliomas show increased lactate dehydrogenase (LDH) and a shift of the LDH isozyme pattern toward predominance of the muscle type, indicating that pyruvate reduction to lactate is favored over oxidation via the citric acid cycle [Gerhardt et al., 1967; Allen, 1972].

Data on changes in glioma oxygen metabolic rate in response to therapy are scarce. One series of 7 cases treated with radiotherapy plus chemotherapy showed a wide range of change in MRO_2 from before to after therapy, all the way from a 65% increase to a 92% decrease [Ogawa et al., 1988].

Measurements of oxygen metabolism with PET in gliomas may not be very useful simply because the dominant energy source, glucose, undergoes glycolysis to lactate rather than oxidative breakdown. Measurements of glucose metabolism are more revealing of tumor tissue energetics than are oxygen measurements.

Hypoxia

Oxygenation is especially important to understand in malignant gliomas because spontaneous necrosis suggests the presence of hypoxic regions resistant to radiotherapy. Low oxygen levels are associated with persistent tumor following radiotherapy and with the subsequent development of local recurrences [Brizel et al., 1999]. Glioblastomas contained hypoxic regions in 10 patients studied with polarographic electrodes [Rampling et al., 1994]. The percent pO_2 values below a hypoxia cutoff were 10–69% with a median of 40%. In four patients with anaplastic astrocytoma the percentage of values below the cutoff were 9–42 with a median of 20%.

The significance of hypoxia in the response of gliomas to radiotherapy needs further clarification. Attempts to eradicate hypoxic cell populations with radiotherapy have been either unsuccessful for hypoxic cell radiosensitizers [Davis, 1989] or too toxic, as reported following fast neutron therapy [Griffin et al., 1983].

In the mid 1980's it was discovered that derivatives of the radiosensitizing drug, misonidazole, are selectively bound to molecules in viable hypoxic cells [Chapman et al., 1998]. This led to the development of [^{18}F]fluoromisonidazole (FMISO) as a hypoxia PET imaging agent [Mathias et al., 1987; Koh et al., 1995]. Reports of FMISO-PET imaging of gliomas are emerging. FMISO was taken up in 14/18 brain tumors [Liu et al., 1999]. In 13 newly-diagnosed patients studied prior to surgery with both FMISO and FDG there was a correlation between FMISO uptake and tumor grade and all high grade lesions showed uptake that was frequently heterogenous [Scott et al., 2001]. There was only partial overlap between regions of FMISO uptake and FDG uptake.

Imaging the hypoxic state of glioblastomas leads to an opportunity to map an important mechanism of resistance to radiotherapy and chemotherapy, and to follow this measure of tumor pathophysiology through the course of therapy and at the time of inevitable recurrence. Identifying the regional distribution of hypoxia may improve planning of resections and allow targeting higher doses of radiotherapy more precisely to the hypoxic areas, similar to the approach we explored wherein a 20 Gy boost was delivered to the volume of FDG uptake [Tralins et al., in press].

IMPROVED APPROACHES TO MOLECULAR IMAGING OF BRAIN TUMORS

When gliomas are in or near gray matter, it can be difficult to distinguish between the two with FDG-PET. We hypothesized that delineation of malignant gliomas from gray matter could be improved by extending the interval between FDG administration and PET data acquisition [Spence et al., 2002b]. Fifteen adult patients with supratentorial gliomas were imaged with FDG-PET as late as 500 min post-injection. The images of all patients were analyzed visually and by calculation of the standard uptake values (SUV) in tumor and gray matter. In 10 of the 15 patients, the delayed images showed better delineation of the high uptake of tumors relative to gray matter (Fig. 3). In twelve patients that had dynamic imaging, the dephosphorylation rate constant (k4) at 90 min was less than at later times in gray matter and tumor. The underestimation of k4 using 90 min data was more striking for the gray matter. This result likely stems from a greater effect of glucose-6-phosphatase degradation of FDG-6-P in normal brain relative to the gliomas.

Energy metabolism and the hypoxic state are important components of the pathophysiology of gliomas on which molecular imaging is providing regional biological information that is clinically relevant. Further advances with potentially useful clinical applications of PET are on the horizon. Proliferation can be assessed with 2-[^{11}C]thymidine or [^{18}F]3′deoxy-3′-fluorothymidine (FLT) [Eary et al., 1999; Sloan et al., 2001]. The former requires metabolite analysis and mathematical modeling of dynamic data [Wells et al., 2002a, b]. FLT is less complicated with respect to metabolite production but may require modeling and dynamic imaging to distinguish retention in the DNA synthetic pathway from uptake as a consequence of blood-brain-barrier disruption. While cell division is the most distinguishing function of growth in tumors, another important process that occurs simultaneously is membrane biosynthesis. This may be assessed with PET and [1-^{11}C]acetate or a choline tracer, [^{11}C]choline or [^{18}F]fluorocholine [DeGrado et al., 2001; Ohtani et al., 2001; Yoshimoto et al., 2001]. Since astrocytic gliomas frequently carry epidermal growth factor receptor (EGFR) mutations at a frequency that is related to grade, a PET tracer specific for this mutated receptor could be very useful clinically for grading and prognosis [Fredriksson et al., 1999]. Methods for imaging angiogenesis are being developed as ^{18}F-labeling of a cyclic RGD-containing glycopeptide, cyclo(-Arg-Gly-Asp-D-Phe-Lys(sugar amino acid)-), with 4-nitrophenyl 2-[^{18}F]fluoropropionate has been reported [Haubner et al., 2001]. [^{18}F]-labeled annexin V is being tested as a new PET agent for quantitating tumor cell

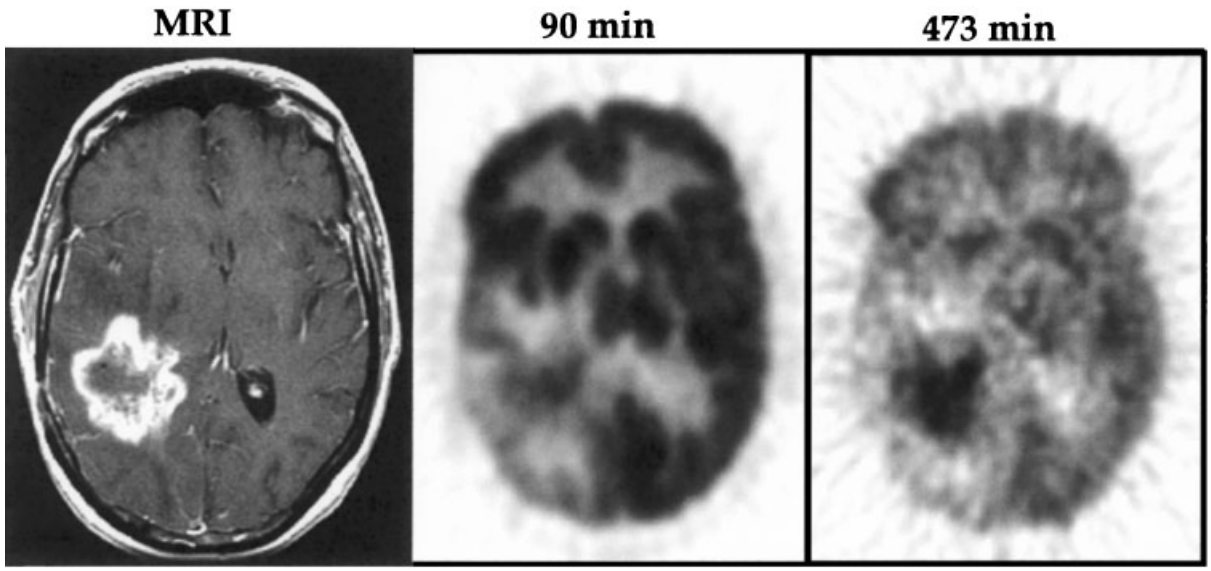

Fig. 3. FDG images from a 46 year-old woman with a recurrent right temporal glioblastoma multiforme. At the later time the tumor is much more prominent relative to gray matter than at the earlier time.

death and predicting response to therapy. Annexin V binds to surface membranes that have exposed phosphatidyl serine residues resulting from programmed cell destruction. Recently, a Tc-99m-labeled derivative has been shown to accumulate in late stage lung cancer and lymphoma in response to chemotherapy [Belhocine et al., 2002].

CONCLUSION

The field of molecular imaging of brain tumors has reached a very high level, but many opportunities lie ahead to integrate our understanding of tumor molecular biology and physiology with our increasingly sophisticated ability to image these processes in vivo and incorporate the imaging measurements into more effective treatment designs.

REFERENCES

Alger JR, Frank JA, Bizzi A, Fulham MJ, DeSouza BX, Duhaney MO, Inscoe SW, Black JL, van Zijl PC, Moonen CT. 1990. Metabolism of human gliomas: Assessment with H-1 MR spectroscopy and F-18 fluorodeoxyglucose PET. Radiology 177:633–641.

Allen N. 1972. Respiration and oxidative metabolism of brain tumors. In: Kirsch WM, Paoletti EG, Paoletti P, editors. The Experimental Biology of Brain Tumors. Springfield; Charles C Thomas. pp 243–274.

Barker FG, Chang SM, Valk PE, Pounds TR, Prados MD. 1997. 18-Fluorodeoxyglucose uptake and survival of patients with suspected recurrent malignant glioma. Cancer 79:115–126.

Baron JC, Rougemont D, Soussaline F, Bustany P, Crouzel C, Bousser MG, Comar D. 1984. Local interrelationships of cerebral oxygen consumption and glucose utilization in normal subjects and in ischemic stroke patients: A positron tomography study. J Cerebral Blood Flow Metab 4:140–149.

Belhocine T, Steinmetz N, Hustinx R, Bartsch P, Jerusalem G, Seidel L, Rigo P, Green A. 2002. Increased uptake of the apoptosis-imaging agent 99mTc recombinant human annexin V in human tumors after one course of chemotherapy as a predictor of tumor response and patient prognosis. Clin Cancer Res 8:2766–2774.

Bennett MJ, Timperley WR, Taylor CB, Hill AS. 1978. Isoenzymes of hexokinase in the developing, normal and neoplastic human brain. Eur J Cancer 14:189–193.

Brizel DM, Dodge RK, Clough RW, Dewhirst MW. 1999. Oxygenation of head and neck cancer: Changes during radiotherapy and impact on treatment outcome. Radiother Oncol 53:113–117.

Burrows RC, Freeman SD, Charlop AW, Wiseman RW, Adamson TCH, Krohn KA, Spence AM. 2002. [^{18}F]-2-fluoro-2-deoxyglucose transport kinetics as a function of extracellular glucose concentration in malignant glioma, fibroblast, and macrophage cells in vitro. Nucl Med Biology submitted.

Chapman JD, Engelhardt EL, Stobbe CC, Schneider RF, Hanks GE. 1998. Measuring hypoxia and predicting tumor radioresistance with nuclear medicine assays. Radiother Oncol 46:229–237.

Crane PD, Pardridge WM, Braun LD, Nyerges AM, Oldendorf WH. 1981. The interaction of transport and metabolism on brain glucose utilization: A reevaluation of the lumped constant. J Neurochem 36:1601–1604.

Curran WJJ, Scott CB, Horton J, Nelson JS, Weinstein AS, Fischbach AJ, Chang CH, Rotman M, Asbell SO, Krisch RE, Nelson DF. 1993. Recursive partitioning analysis of prognostic factors in three Radiation Therapy Oncology Group malignant glioma trials. J Natl Cancer Inst 85: 704–710.

Davis LW. 1989. Malignant glioma—A nemesis which requires clinical and basic investigation in radiation oncology. Int J Radiat Oncol Biol Phys 16:1355–1365.

De Witte O, Hildebrand J, Luxen A, Goldman S. 1994. Acute effect of carmustine on glucose metabolism in brain and glioblastoma. Cancer 74:2836–2842.

DeGrado TR, Baldwin SW, Wang S, Orr MD, Liao RP, Friedman HS, Reiman R, Price DT, Coleman RE. 2001. Synthesis and evaluation of (18)F-labeled choline analogs as oncologic PET tracers. J Nucl Med 42:1805–1814.

Di Chiro G. 1987. Positron emission tomography using [^{18}F] fluorodeoxyglucose in brain tumors: A powerful diagnostic and prognostic tool. Invest Radiol 22:360–371.

Di Chiro G, Brooks RA. 1988. PET quantitation: Blessing and curse. J Nucl Med 29:1603–1604.

Doenst T, Taegtmeyer H. 1998. Complexities underlying the quantitative determination of myocardial glucose uptake with 2-deoxyglucose. J Mol Cell Cardiol 30:1595–1604.

Eary JF, Mankoff DA, Spence AM, Berger MS, Olshen A, Link JM, O'Sullivan F, Krohn KA. 1999. 2-[C-11]thymidine imaging of malignant brain tumors. Cancer Res 59: 615–621.

Fredriksson A, Johnstrom P, Thorell JO, von Heijne G, Hassan M, Eksborg S, Kogner P, Borgstrom P, Ingvar M, Stone-Elander S. 1999. In vivo evaluation of the biodistribution of 11C-labeled PD153035 in rats without and with neuroblastoma implants. Life Sci 65:165–174.

Fujibayashi Y, Waki A, Sakahara H, Konishi J, Yonekura Y, Ishii Y, Yokoyama A. 1997. Transient increase in glycolytic metabolism in cultured tumor cells immediately after exposure to ionizing radiation: From gene expression to deoxyglucose uptake. Radiat Res 147:729–734.

Furuta M, Hasegawa M, Hayakawa K, Yamakawa M, Ishikawa H, Nonaka T, Mitsuhashi N, Niibe H. 1997. Rapid rise in FDG uptake in an irradiated human tumour xenograft. Eur J Nucl Med 24:435–438.

Gaitonde MK, Evison E, Evans GM. 1983. The rate of utilization of glucose via hexosemonophosphate shunt in brain. J Neurochem 41:1253–1260.

Gerhardt W, Clausen J, Christensen E, Riishede J. 1967. Lactate dehydrogenase isoenzymes in the diagnosis of human benign and malignant brain tumors. J Natl Cancer Inst 38:343–357.

Graham MM, Muzi M, Spence AM, O'Sullivan F, Lewellen TK, Link JM, Krohn KA. 2002. The fluorodeoxyglucose lumped constant in normal human brain. J Nucl Med 43:1157–1166.

Griffin TW, Davis R, Laramore G, Hendrickson F, Rodrigues Antunez A, Hussey D, Nelson J. 1983. Fast neutron radiation therapy for glioblastoma multiforme. Results of an RTOG study. Am J Clin Oncol 6:661–667.

Haberkorn U, Morr I, Oberdorfer F, Bellemann ME, Blatter J, Altmann A, Kahn B, van Kaick G. 1994. Fluorodeoxyglucose uptake in vitro: Aspects of method and effects of treatment with gemcitabine. J Nucl Med 35:1842–1850.

Hasegawa M, Mitsuhashi N, Yamakawa M, Furuta M, Maebayashi K, Imai R, Hayakawa K, Niibe H. 1997. p53 protein expression and radiation-induced apoptosis in human tumors transplanted to nude mice. Radiat Med 15:171–176.

Haubner R, Wester HJ, Weber WA, Mang C, Ziegler SI, Goodman SL, Senekowitsch-Schmidtke R, Kessler H, Schwaiger M. 2001. Noninvasive imaging of alpha(v)-beta3 integrin expression using ^{18}F-labeled RGD-containing glycopeptide and positron emission tomography. Cancer Res 61:1781–1785.

Herholz K, Heindel W, Luyten PR, den Hollander JA, Pietrzyk U, Voges J, Kugel H, Friedmann G, Heiss WD. 1992. In vivo imaging of glucose consumption and lactate concentration in human gliomas. Ann Neurol 31:319–327.

Hoekstra CJ, Paglianiti I, Hoekstra OS, Smit EF, Postmus PE, Teule GJ, Lammertsma AA. 2000. Monitoring response to therapy in cancer using [^{18}F]-2-fluoro-2-deoxy-D-glucose and positron emission tomography: An overview of different analytical methods. Eur J Nucl Med 27:731–743.

Holzer T, Herholz K, Jeske J, Heiss WD. 1993. FDG-PET as a prognostic indicator in radiochemotherapy of glioblastoma. J Comput Assist Tomogr 17:681–687.

Hossmann KA, Mies G, Paschen W, Szabo L, Dolan E, Wechsler W. 1986. Regional metabolism of experimental brain tumors. Acta Neuropathol Berl 69:139–147.

Koh WJ, Bergman KS, Rasey JS, Peterson LM, Evans ML, Graham MM, Grierson JR, Lindsley KL, Lewellen TK, Krohn KA. 1995. Evaluation of oxygenation status during fractionated radiotherapy in human nonsmall cell lung cancers using [F-18]fluoromisonidazole positron emission tomography. Int J Radiat Oncol Biol Phys 33: 391–398.

Kubota R, Yamada S, Kubota K, Ishiwata K, Tamahashi N, Ido T. 1992. Intratumoral distribution of fluorine-18-fluorodeoxyglucose in vivo: High accumulation in macrophages and granulation tissues studied by microautoradiography. J Nucl Med 33:1972–1980.

Lee SW, Fraass BA, Marsh LH, Herbort K, Gebarski SS, Martel MK, Radany EH, Lichter AS, Sandler HM. 1999. Patterns of failure following high-dose 3-D conformal radiotherapy for high-grade astrocytomas: A quantitative dosimetric study. Int J Radiat Oncol Biol Phys 43: 79–88.

Liu RS, Chu LS, Chu YK, Yen SH, Liao SQ, Yeh SH. 1999. Does β-oxidation occur in malignant neoplasm? A concurrent [C-11]acetate and [F-18]MISO study (abstract). J Nucl Med 40(suppl):239p.

Maruyama I, Sadato N, Waki A, Tsuchida T, Yoshida M, Fujibayashi Y, Ishii Y, Kubota T, Yonekura Y. 1999. Hyperacute changes in glucose metabolism of brain tumors after stereotactic radiosurgery: A PET study. J Nucl Med 40:1085–1090.

Mathias CJ, Welch MJ, Kilbourn MR, Jerabek PA, Patrick TB, Raichle ME, Krohn KA, Rasey JS, Shaw DW. 1987. Radiolabeled hypoxic cell sensitizers: Tracers for assessment of ischemia. Life Sci 41:199–206.

Muzi M, Freeman SD, Burrows RC, Wiseman RW, Link JM, Krohn KA, Graham MM, Spence AM. 2001. Kinetic characterization of hexokinase isoenzymes from glioma cells: Implications for FDG imaging of human brain tumors. Nucl Med Biol 28:107–116.

Ogawa T, Uemura K, Shishido F, Yamaguchi T, Murakami M, Inugami A, Kanno I, Sasaki H, Kato T, Hirata K, Kowada M, Mineura K, Yasuda T. 1988. Changes of cerebral blood flow and oxygen and glucose metabolism following radiochemotherapy of gliomas: A PET study. J Comput Assist Tomogr 12:290–297.

Ohtani T, Kurihara H, Ishiuchi S, Saito N, Oriuchi N, Inoue T, Sasaki T. 2001. Brain tumour imaging with carbon-11 choline: Comparison with FDG PET and gadolinium-enhanced MR imaging. Eur J Nucl Med 28:1664–1670.

Oudard S. 1996. High glycolysis in gliomas despite low hexokinase transcription and activity correlated with chromosome 10 loss. Br J Cancer 74:839–845.

Oudard S, Poirson F, Miccoli L, Bourgeois Y, Vassault A, Poisson M, Magdelenat H, Dutrillaux B, Poupon MF. 1995. Mitochondria-bound hexokinase as target for therapy of malignant gliomas. Int J Cancer 62:216–222.

Padma MV, Said S, Jacobs M, Hwang DR, Dunigan K, Christian B, Satter M, Bernstein T, Kraus G, Mantil JC. 2002. Prediction of pathology and survival by ^{18}F-FDG PET in gliomas. J Nucl Med 43:111P.

Patronas NJ, Di Chiro G, Kufta C, Bairamian D, Kornblith PL, Simon R, Larson SM. 1985. Prediction of survival in glioma patients by means of positron emission tomography. J Neurosurg 62:816–822.

Rampling R, Cruickshank G, Lewis AD, Fitzsimmons SA, Workman P. 1994. Direct measurement of pO_2 distribution and bioreductive enzymes in human malignant brain tumors. Int J Radiat Oncol Biol Phys 29:427–431.

Reinhardt MJ, Kubota K, Yamada S, Iwata R, Yaegashi H. 1997. Assessment of cancer recurrence in residual tumors after fractionated radiotherapy: A comparison of fluorodeoxyglucose, L-methionine, and thymidine. J Nucl Med 38:280–287.

Rhodes CG, Wise RJ, Gibbs JM, Frackowiak RS, Hatazawa J, Palmer AJ, Thomas DG, Jones T. 1983. In vivo disturbance of the oxidative metabolism of glucose in human cerebral gliomas. Ann Neurol 14:614–626.

Scott AM, Ramdave S, Hannah A, Pathmaraj K, Tochon-Danguy H, Sachinidis J, Chan J, Berlangieri SU, Fabinyi G, Cher LM. 2001. Correlation of hypoxic cell fraction with glucose metabolic rate in gliomas with ^{18}F-fluoromisonidazole (FMISO) and ^{18}F-fluorodeoxyglucose (FDG) positron emission tomography (PET). J Nucl Med (Abstract 250) 42:267P.

Sloan AE, Shields AF, Kupsky W, Heilbrun N, Abrams J, Barger G, Kuntzsch M, Reimold M, Machulla H-J, Bares R. 2001. Superiority of [F-18]FLT-PET compared to FDG PET in assessing proliferative activity and tumor physiology in primary and recurrent intracranial gliomas. Neuro-Oncology (Abstract 313) 3:345.

Smith TA, Maisey NR, Titley JC, Jackson LE, Leach MO, Ronen SM. 2000. Treatment of SW620 cells with Tomudex and oxaliplatin induces changes in 2-deoxy-D-

glucose incorporation associated with modifications in glucose transport. J Nucl Med 41:1753–1759.

Sokoloff L. 1981. The deoxyglucose method: Theory and practice. Eur Neurol 20:137–145.

Sokoloff L, Reivich M, Kennedy C, Des Rosiers MH, Patlak CS, Pettigrew KD, Sakurada O, Shinohara M. 1977. The [14C]deoxyglucose method for the measurement of local cerebral glucose utilization: Theory, procedure, and normal values in the conscious and anesthetized albino rat. J Neurochem 28:897–916.

Spence AM, Graham MM, Abbott GL, Muzi M, Krohn KA, Kapoor R. 1988. Assessment of deoxyglucose and glucose transport in a rat transplanted brain tumor model. J Nucl Med 29:920.

Spence AM, Graham MM, Muzi M, Freeman SD, Link JM, Grierson JR, O'Sullivan F, Stein D, Abbott GL, Krohn KA. 1997. Feasibility of imaging pentose cycle glucose metabolism in gliomas with PET: Studies in rat brain tumor models. J Nucl Med 38:617–624.

Spence AM, Muzi M, Graham MM, O'Sullivan F, Krohn KA, Link JM, Lewellen TK, Lewellen B, Freeman SD, Berger MS, Ojemann GA. 1998. Glucose metabolism in human malignant gliomas measured quantitatively with PET, 1-[C-11]glucose, and FDG: Analysis of the FDG lumped constant. J Nucl Med 39:440–448.

Spence AM, Muzi M, Graham MM, O'Sullivan F, Link JM, Lewellen TK, Lewellen B, Freeman SD, Mankoff DA, Eary JF, Krohn KA. 2002a. FDG and glucose uptake in malignant gliomas before and after radiotherapy: Correlation with outcome. Clinical Cancer Res 8:971–979.

Spence AM, Muzi M, O'Sullivan F, Mankoff DA, Minoshima S, Krohn KA. 2002b. FDG-PET of malignant gliomas at delayed intervals: Improved distinction between tumor and gray matter. 49th Annual Meeting of the Society of Nuclear Medicine. Los Angeles.

Tralins KS, Douglas JG, Stelzer KJ, Mankoff DA, Silbergeld DL, Rostomily R, Hummel S, Scharnhorst J, Krohn KA, Spence AM. Volumetric analysis of fluorodeoxyglucose positron emission tomography in glioblastoma multiforme: prognostic information and possible role in definition of target volumes in radiation dose escalation. J Nucl Med (in press).

Wells JM, Mankoff DA, Eary JF, Spence AM, Muzi M, O'Sullivan F, Vernon CB, Link JM, Krohn KA. 2002a. Kinetic analysis of 2-[11C]Thymidine PET imaging studies of malignant brain tumors—Preliminary patient results. Molecular Imaging (in press).

Wells JM, Mankoff DA, Muzi M, O'Sullivan F, Eary JF, Spence AM, Krohn KA. 2002b. Kinetic analysis of 2-[11C]Thymidine PET imaging studies of malignant brain tumors: Compartmental model investigation and mathematical analysis. Molecular Imaging. (in press).

Wise RJS, Thomas DGT, Lammertsma AA, Rhodes CG. 1984. PET scanning of human brain tumors. Prog Exp Tumor Res 27:154–169.

Yoshimoto M, Waki A, Yonekura Y, Fujibayashi Y. 2001. Acetate and choline as cell growth markers provide different perspectives of lipid synthesis. J Nucl Med 42: 275p.